PREDICTION OF GRAIN BOUNDARY EVOLUTION IN AN TITANIUM ALLOY SUBSTRATE USING A NOVEL PHASE FIELD MODEL COUPLED WITH A SEMI-ANALYTICAL THERMAL SOLUTION

T. F. FLINT*, Q. XIONG* Y. L. SUN*, A. N. VASILEIOU*, M. C. SMITH* and J. A. FRANCIS*

** Dalton Nuclear Institute, The University of Manchester, Manchester M13 9PL, UK*
Corresponding Author - Thomas.flint@manchester.ac.uk (Orcid: 0000-0002-0615-8621)

DOI 10.3217/978-3-85125-615-4-45

ABSTRACT

Grain boundary migration in the presence of concentrated sources of heat is a complex process that has a considerable impact on resultant material properties. The large thermal gradients generated during welding cause grain boundaries to migrate in order to minimise the total free energy of the system. It is important to consider both the thermal gradient driving force, as well as the local curvature driving force of the grain boundaries which both play a significant role in the evolution of the micro-structure in the weld region. In this work a multi-phase field model is used to predict the grain boundary evolution in a Ti6Al4V substrate subjected to a heat source representative of the electron beam (EB) welding process. While numerical simulations incorporating the mass transfer and complex flow dynamics associated with high energy density welding processes are favourable in that they consider the physical processes occurring in the weld explicitly, they are also extremely computationally expensive. As such, the thermal field, on which the phase field model is dependent, is computed using a semi-analytical solution technique. In this approach the complicated flow dynamics of the EB process are represented as a four-quadrant volumetric heat source, the recently published DEC heat source which has shown to be a good thermal representation of EB processes. Using a Green's function approach, the time and position dependent thermal field is obtained for this DEC heat source in motion is found, free from numerical errors. Predicted grain size distributions are presented for various energy inputs and conclusions drawn based on the applied driving forces, captured in the phase field model

Keywords: Phase Field; High Energy Density; Analytical Solution; Grain Boundary Migration; Thermal Gradient

INTRODUCTION

Grain boundaries in alloy systems migrate in response to driving forces acting upon them, in such a manner as to minimise the total free energy in the entire system [14, 13]. The resultant micro structure has strong effects on the physical properties and may favourably or adversely affect material performance and is therefore of great academic and industrial interest [5, 9, 7]. Recently, the effect of thermal gradient and curvature driving forces has been studied for an isotropic micro structure. It has been shown that the thermal gradient driving force is an important factor in determining the coarsening behaviour local to high energy density sources of heat, as are present in advanced manufacturing processes [5]. The thermal field induced in a domain may be calculated using a full thermal fluid dynamics approach; where the complex heat and mass transfer involved in the EB welding process was fully resolved and the physics fully captured for the most accurate prediction of the thermal fields and their spatial gradients [12]. While the thermal fluid dynamics approach is preferred, the computational cost is high. In this respect it is beneficial to use a semi-analytical solution procedure to calculate the thermal fields.

In this semi-analytical approach, the complex flow dynamics of the molten and vaporised substrate material is represented as a volumetric heat flux distribution. The most representative volumetric heat source model for high energy density welding processes is the double ellipsoidal conical (DEC) heat source model which was recently proposed [3]. With this approach the momentum equations are not explicitly solved, and the complex physics of the process is captured in the heat flux model. This semi-analytical approach has shown to be promising in the limiting case where the component geometry is orthogonal [2, 6]. Recently a semi-analytical solution was computed for the (DEC) heat source model using a Green's function approach and the method of images for construction of Dirichlet and/or Neumann boundary conditions [4]. The nature of the Greens function approach for the construction of the semi-analytical solution enables multiple heat sources to be considered. This ensures that the typical 'bugle' type fusion profile in EB welds is achieved [4]. A major advantage of the semi-analytical solution approach is that the entire domain of the weld under consideration need not be considered to compute the temperature history at a given set of points, this is attractive for the investigation of micro structural behaviour, due to complex thermal histories, at specific locations.

In this work the semi-analytical approach is used for the computationally efficient, yet physically justified, calculation of the thermal field induced in a Ti6Al4V substrate due to the application of a high energy density beam of electrons causing melting and vaporisation. The micro structural evolution in the substrate is predicted using a multi-phase field model considering boundary curvature and thermal gradient driving forces at grain interfaces. The computational domain for the simulations is placed in the heat affected zone (HAZ) of the Ti6Al4V substrate such that no state change is considered in the metallic substrate. The effect of welding travel speed on micro-structural evolution is investigated with conclusions drawn based on the physical justification of the chosen multi-phase field model.

SOLUTION APPROACH

To predict the evolution of the temperature field due to a complex heat source and the evolution of the micro structure that this thermal field initiates; appropriate physical models and numerical techniques must be used. The multi-phase field model has been chosen for

the simulation of the micro structural evolution as it is able to physically resolve important thermodynamic driving forces at the grain boundaries that determine migration behaviour. The semi-analytical solution approach for the computation of the transient temperature fields has been chosen due to the unparalleled computational efficiency the approach offers, and the generation of a thermal field free from spatial numerical discretisation errors.

MULTI-PHASE FIELD MODEL

To predict the micro structural behaviour of the material under consideration a physics-based model, such as the phase-field model, should be used. This type of model incorporates various driving forces into the free energy functional of the system and can accurately predict the micro structural behaviour due to complex thermal fields. The velocity, v, of a migrating grain boundary is given as the superposition of the curvature driving pressure, F_c, and the thermal gradient driving pressure, F_t as shown in Equation 1

$$v = m(Ft + Fc) = m(\frac{\Delta S 2\lambda \nabla T}{\Omega} - \sigma\kappa) \tag{1}$$

where m is the GB mobility, κ is the local curvature, ΔS is the entropy difference between the GB and the crystal which is approximately equal to the melting entropy, 2λ is the GB width, T is the temperature and Ω is the molar volume of the material and σ is the GB energy. [10, 7, 1]. In this work T is computed using the semi-analytical approach due to the application of a DEC heat flux in the heat equation. The evolution equation for the PF is then given by Equation 2

$$\frac{\partial \varphi_n}{\partial t} = \frac{2M_\varphi}{S} \sum_{p \neq n}^{N} s_p \, s_n \left(\frac{\delta F}{\delta \varphi_n} - \frac{\delta F}{\delta \varphi_p} \right) \tag{2}$$

where M_φ is the isotropic PF mobility [10, 14], and has the form $M_\varphi = {m\sigma}/{\epsilon^2} = {\pi^2 m}/{16\xi}$. The parameters S and s are used to define the sum of the number of coexisting phases and a step function per phase respectively. m is strongly temperature dependent and is often assumed to follow an Arrhenius-type relationship as shown in Equation 3.

$$m = m_0 e^{-Q/k_B T} \tag{3}$$

The variation in the free energy density due to the GB curvature and thermal gradient driving forces is given by Equation 4

$$\frac{\delta F}{\delta \varphi_n} = \sum_{m \neq n}^{N} \left(\frac{\varepsilon^2}{2} \nabla^2 \varphi_m + \omega \varphi_m - \frac{\mu}{2} \nabla \varphi_m \cdot \nabla T \right) \tag{4}$$

where ϵ is the gradient energy coefficient, T is the temperature, μ is the temperature gradient energy coefficient, and ω is the height of the parabolic potential with a double obstacle [5, 10]. The parameters ϵ, ω, μ and Mφ have definite relationships with the GB energy, σ, PF boundary width, 2ξ, boundary entropy difference, ΔS, GB width, 2λ, alloy

molar volume, Ω, and mobility m of a GB. Q is the activation energy for the GB under consideration, m_0 is a pre-exponential constant and k_B is the Boltzmann constant.

SEMI-ANALYTICAL SOLUTION FOR THE TRANSIENT TEMPERATURE FIELD

The semi-analytical computation of the temperature field induced by a DEC volumetric heat flux model is performed using a Laplace transform approach as well as the method of images (MOI) to generate analytical expressions for the heat kernels in the spatial dimensions before the final numerical temporal integration is performed [4, 3]. For a 3D domain with insulating boundary conditions on all faces except a Dirichlet boundary condition on the x = B face the three-dimensional Green's function may be found by multiplying the appropriate 1D functions and is shown in Equation 5

$$G = \sum_{n=-\infty}^{\infty} \left\{ \begin{array}{c} (-1^n) \dfrac{e^{-\frac{(2nB+x-x\prime)^2}{4\alpha(t-t\prime)}} + e^{-\frac{(2nB+x+x\prime)^2}{4\alpha(t-t\prime)}}}{\sqrt{4\pi\alpha(t-t\prime)}} \times \\ \dfrac{e^{-\frac{(2nD+y-y\prime)^2}{4\alpha(t-t\prime)}} + e^{-\frac{(2nD+y+y\prime)^2}{4\alpha(t-t\prime)}}}{\sqrt{4\pi\alpha(t-t\prime)}} \times \\ \dfrac{e^{-\frac{(2nL+z-z\prime)^2}{4\alpha(t-t\prime)}} + e^{-\frac{(2nL+z+z\prime)^2}{4\alpha(t-t\prime)}}}{\sqrt{4\pi\alpha(t-t\prime)}} \end{array} \right\} \tag{5}$$

where $\alpha = \frac{k}{\rho c_p}$ is the thermal diffusivity; k is the thermal conductivity, ρ is the mass density and c_p is the specific heat at constant pressure respectively. The temperature variation induced at a point with co-ordinates (x,y,z) at a time t, by an instantaneous heat pulse of magnitude $q_{(x',y',z',t')}$ is then $\frac{1}{\rho c_p} q_{(x',y',z',t')} G_{(x,x',y,y',z,z',t,t')}$. The temperature increment at point (x,y,z,t) is given by the integral over time as shown in Equation 6

$$\frac{1}{\rho c_p} \times \int_0^t q_{(x',y',z',t')} G_{(x,x',y,y',z,z',t,t')} dt' \tag{6}$$

The temperature increase at any point and time, t, due to a volumetric heat source $q_{(x',y',z',t')}$ is given by Equation 7

$$\Delta T_{(x,y,z,t)} = \frac{1}{\rho c_p} \times \int_0^t \int_0^L \int_0^D \int_0^B q_{(x',y',z',t')} G_{(x,x',y,y',z,z',t,t')} \, dx'dy'dz'dt' \tag{7}$$

Here $q_{(x',y',z',t')}$ represents the DEC heat source distribution as shown in Figure 1, where a surface of constant power density is displayed, and the spatial parameters of the heat source are shown. The functional form of the DEC distribution is fully described elsewhere [3].

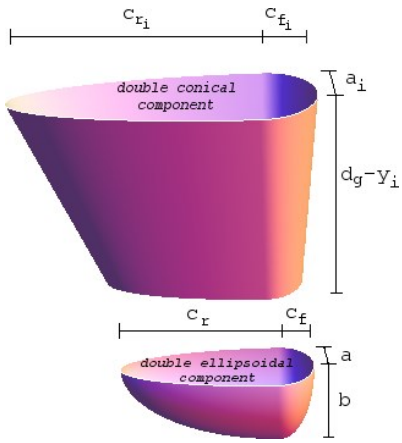

Fig. 1 A schematic representation of the double ellipsoidal conical heat source model showing the spatial parameters

The transient thermal field induced in the finite domain due to the DEC heat source distribution is computed by summing the contributions from the four quadrants of the DEC heat source according to Equation 8 where the spatial integration's have been performed after collecting the dimensional components. The minutia of the computation of the semi-analytical thermal solution is detailed elsewhere, including the spatial heat kernels BX, DX and LX [4, 3].

$$\Delta T_{(x,y,z,t)} = \frac{1}{\rho c_p} \times \int_0^t \left\{ \begin{array}{l} \left(Q_{0_{Cr}} B_T D_{T_c} L_{T_r}\right) + \left(Q_{0_{Cf}} B_T D_{T_c} L_{T_f}\right) + \\ \left(Q_{0_{Dr}} B_T D_{T_e} L_{T_r}\right) + \left(Q_{0_{Df}} B_T D_{T_e} L_{T_f}\right) \end{array} \right\} dt' \tag{8}$$

In the semi-analytical approach, multiple heat sources may be applied. In approaches where momentum and mass transfer effects are neglected, typically the predicted fusion zone profiles are not appropriate due to neglecting surface flow effects. To compensate for this a small surface heat source may be added to represent the thermal contribution due to the mass and heat transfer sue to this flow at the surface [4]. The thermal contribution from the surface Gaussian distribution is computed according to Equation 9, where a is the radius of the surface Gaussian distribution, and f is the heat fraction apportioned to the surface distribution.

$$\frac{6f\sqrt{3}P}{\rho c_p a^3 \pi \sqrt{\pi}} \times \int_0^t B_T D_{T_{e(d_g=0)}} \left(L_{T_{r(c_r=a)}} + L_{T_{f(c_f=a)}}\right) dt' \tag{9}$$

where P is the power of the electron beam heat source, generally taken as the product of the current, voltage and efficiency of the source. The temperature at any point within the finite domain is given by the sum of Equation 8 and Equation 9. Figure 2 shows the computed temperature field and spatial derivatives for an arbitrary EB welding geometry as the heat source model is at peak intensity through the cross section. The temperature and

spatial derivatives are then used in the phase field model to determine the evolution behavior of the order parameters φ_n.

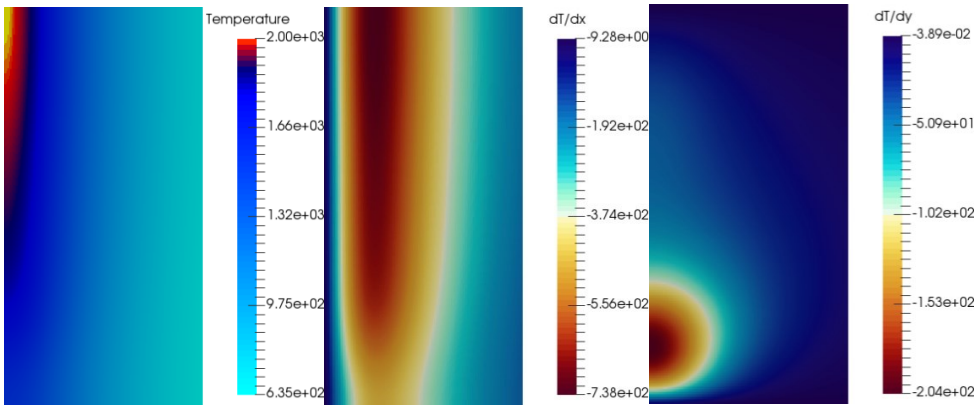

Fig. 2 Representative temperature field as computed by Equations 8 and 9 and spatial derivatives that are used in the multi-phase field analysis off the micro-structural evolution.

RESULTS AND DISCUSSION

In this work, initially a small numerical study was performed to investigate the effects of the phase field interface width on the boundary migration velocity for a linear boundary in a constant thermal gradient. Once an appropriate width had been determined, the effect of welding travel speed on microstructural evolution was investigated for a two-dimensional region in the HAZ of a Ti6Al4V substrate.

SINGLE LINEAR BOUNDARY IN A CONSTANT THERMAL GRADIENT

A key parameter in the phase field model is the boundary width, 2ξ, this has a strong influence on the response of the boundaries to applied driving forces. To determine an appropriate value a small numerical study was performed to determine the optimum value of the phase field width. The remaining parameters used in the phase field simulation are shown in Table 1 [8].

Table 1 Values and units of the parameters used in the multi-phase field simulations

Parameter	Value
$\sigma(kg\ s^{-2})$	0.81
$\Omega(mm^3 mol^{-1})$	100.3×10^3
$\Delta S(kg\ mm^2\ s^{-1}K^{-1}mol^{-1})$	152.9×10^6
$Q(eV)$	1.0
$2\lambda(nm)$	5.0
$m_0(mm^2 kg^{-1}\ s)$	178.0
$\alpha(mm^2\ s^{-1})$	7.06

For various values of ξ, the velocity of the migrating PF boundary was found, for the same inter-facial energy. Figure 3 shows how the PF velocity tended to the analytically determined velocity, deduced from Equation 1, with $\kappa = 0$ as is the case for a linear boundary, in a thermal gradient of $93.9 \times 10^6\ Km^{-1}$.

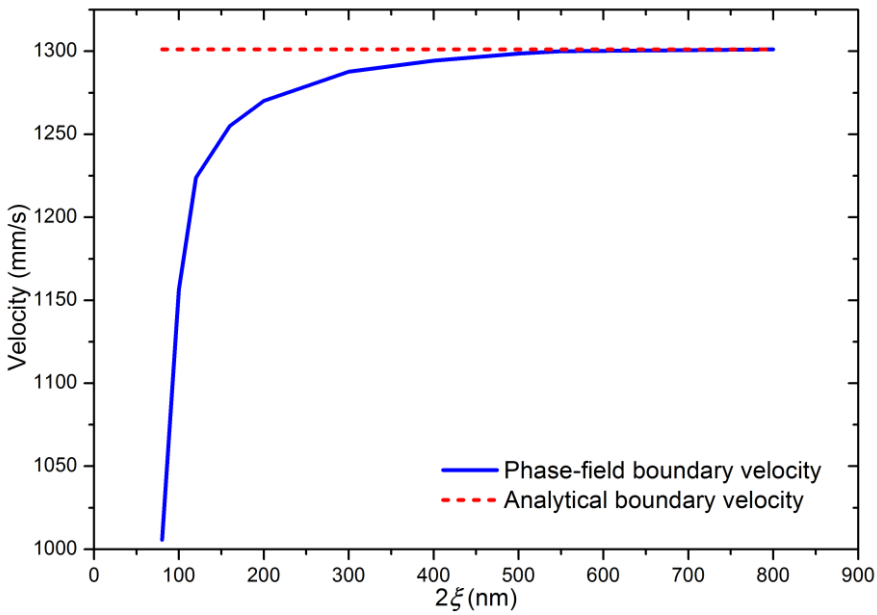

Fig. 3 Velocity of a linear boundary in a constant thermal gradient, as a function of the phase field width parameter. The analytical velocity of a linear boundary normal to this temperature gradient is shown by the red dashed line.

A boundary width of 2ξ = 80 nm, corresponding to 4 calculation points in the simulation domain, resulted in a PF boundary velocity of 1005.7 mm s − 1, an error of 22.70% with respect to the analytical boundary velocity of 1301.1 mm s − 1. A boundary width of 300 nm resulted in a PF velocity of 1287.8 mm s − 1, an error of 1.08%. As the number of cells that the PF boundary spans is increased, the accuracy of the PF simulation increases, as can be seen from Figure 3↑. This single GB simulation was used to determine the value of the width parameter, 2ξ, for the subsequent GB network simulations; boundary widths were chosen such that the PF boundaries spanned a minimum of 10 cells.

THE EFFECT OF WELDING SPEED ON MICROSTRUCTURAL DEVELOPMENT

With the PF model parameters defined the behaviour of a Ti6Al4V substrate subjected to a DEC heat source was considered. A Ti6Al4V plate with dimensions 170mm in the x-direction, 1mm in the y-direction and 300mm in the z-direction was considered. The heat source travelled along the x=85mm plane, the heat source applied normal to the y=0 surface such that the heat source intensity decreased as the distance into the domain increased. The remaining thermal modelling parameters for the semi-analytical solution are the spatial heat flux parameters and the heat source power. The heat source power, P, has a value of 120W. The heat source shape parameters are: $a = a_i = 0.3mm$, $b = 0.2mm$, $c_r = c_{r_i} = 4.0mm$, $c_f = c_{f_i} = 1.0mm$ and $b_g = 85.0mm$. The fraction of heat in the surface Gaussian distribution, f, used was 0.04. The radius of the surface Gaussian component is 0.25mm.

While this work focuses on the grain structure evolution in the HAZ, where no state change occurs, it is interesting to observe the spatial extent of the molten phase within the Ti6Al4V substrate due to the DEC heat source model. Figure 4 shows the cross section through the welding axis for the case under consideration as the heat source is at peak intensity. Above the solidus temperature the phase field variables have assigned a random orientation. The solidus interface is then clearly visible in the phase field domain with the typical ’bugle’ type profile typically seen in high energy density welding scenarios. As can be seen in Figure 4 the grains immediately adjacent to the solid-liquid interface have begun to coarsen due to the strong thermal gradients and curvature driving forces. Away from the heat source location there has been negligible grain coarsening due to the relatively low temperature and the nature of the relation between mobility and temperature.

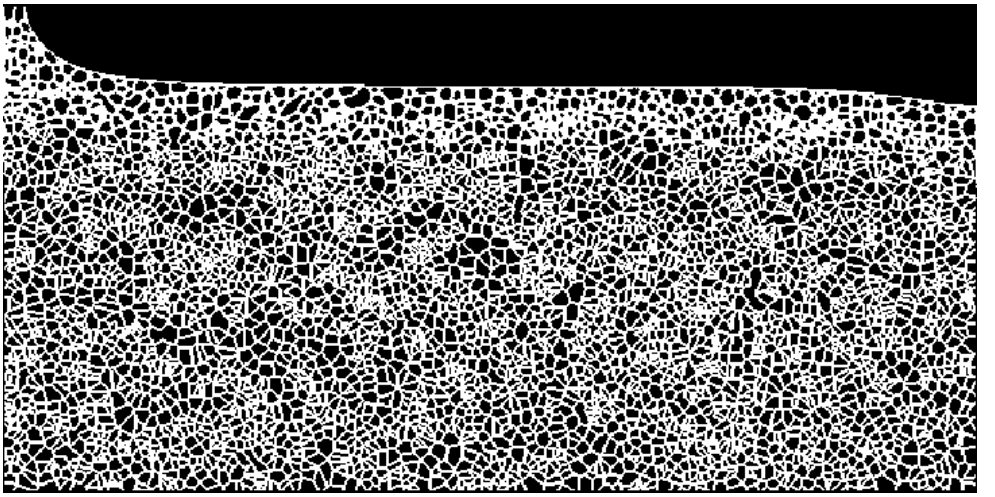

Fig. 4 Cross-section through the welding axis as the DEC heat source traverses the computational domain

A theoretical investigation was performed on a Ti6Al4V substrate subjected to a DEC heat source representative of an EB welding process. The evolution of the micro structure was simulated immediately adjacent to the fusion zone for the duration of the heat source application. Therefore, no consideration of state change in the metallic grains is considered. Figure 5 shows the iso-thermal lines in the heat affected zone considered, as the heat source traverses, for an arbitrary time. To investigate the effect of welding heat source travel speed on microstructural development, a heat source as described was applied to the substrate with a travel speed of 3.33 m/s and a slightly higher speed of 5.0 m/s. The phase field simulation domain considered was a square of side 0.5mm, initialised with 1600 grains at t=0s, representative of the grain size observed in Ti6Al4V alloy systems.

The grain boundaries tend to migrate up the temperature gradient and normal to these lines, if the spatial thermal gradients are of high enough magnitude to be dominant over the curvature driving forces. As the thermal field evolves, the iso-thermal lines migrate and therefore the thermal gradient driving force is a strong function of time.

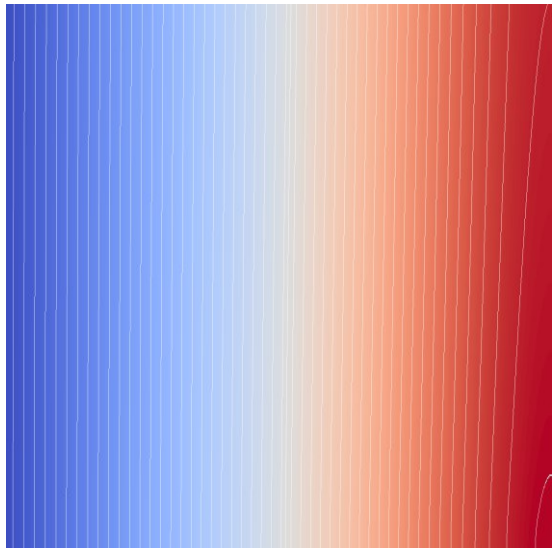

Fig. 5 Time dependent temperature field for an arbitrary time. As the temperature field evolves, as too do the thermal gradients and therefore the magnitude and direction of the thermal gradient driving force

Figure 6 shows the resultant micro structure in the HAZ for the 3.33m/s speed, while Figure 7 shows the same section of the micro structure after the application of the heat source with at velocity of 5.0m/s, at various times after the heat source reaches peak intensity in the considered domain. Both figures show the evolution in the x-z plane perpendicular to the heat source travel direction. The heat source was located at some distance to the east in the chosen cross section as shown in Figure 5.

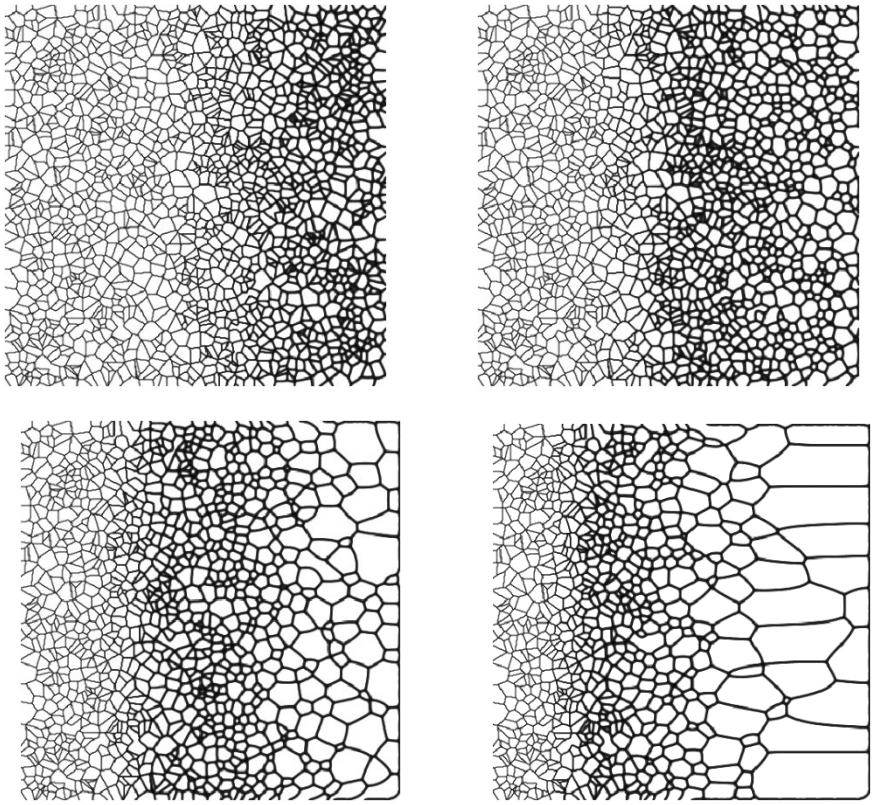

Fig. 6 Evolution of temperature field in the heat affected zone of a full penetration EB weld in Ti6Al4V due to the application of a DEC heat source with surface Gaussian component, at a travel speed of 3.33 m s^{-1}. The images correspond to a cross section through the HAZ perpendicular to the heat source travel vector at 1.375×10^{-4} *s*, 1.375×10^{-3} *s*, 1.375×10^{-2} *s* and 1.375×10^{-1} *s* respectively after the DEC heat flux reaches peak intensity.

The thermal gradient driving force on the right of the sub-figures, where the spatial thermal gradients are largest, has a considerable effect on the development of a columnar grain structure, as can be seen n Figure 6. The lower travel speed of the heat source for the same P deposits more energy into the substrate and means that the average temperature of the domain is higher than in the higher travel speed case. The higher average temperature and steep thermal gradients leads to considerable coarsening and boundary migration towards the hotter region of the domain.

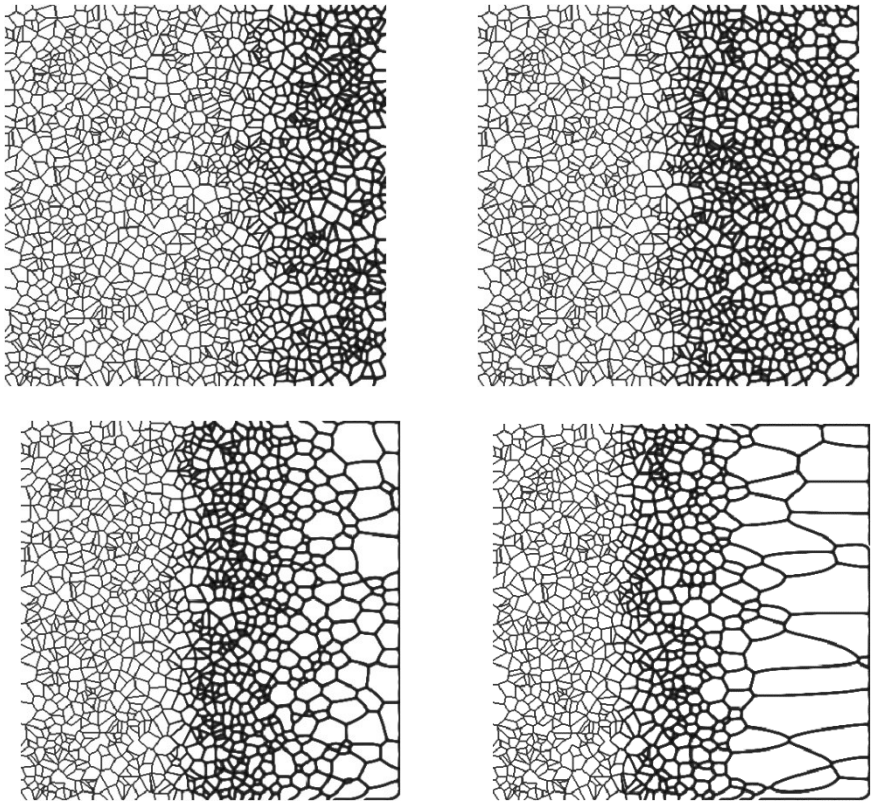

Fig. 7 Evolution of temperature field in the heat affected zone of a full penetration EB weld in Ti6Al4V due to the application of a DEC heat source with surface Gaussian component, at a travel speed of 5.0 m s^{-1}. The images correspond to a cross section through the HAZ perpendicular to the heat source travel vector at 1.375×10^{-4} *s*, 1.375×10^{-3} *s*, 1.375×10^{-2} *s* and 1.375×10^{-1} *s* respectively after the DEC heat flux reaches peak intensity.

In the higher travel velocity case as shown in Figure 7 the temperature on the boundary farthest away from the heat source location doesn't reach as high a magnitude; as such the mobility of the boundaries is lower due to the Arrhenius dependence of the mobility with temperature. There is still considerable boundary migration and coarsening towards the hotter region of the domain. However, comparing Figures 6 and 7 at 1.375×10-1 s after the heat source traversed the plane, more coarsening occurred and the extent of the HAZ is greater in the slower case. This agrees with the expected microstructural behaviour.

CONCLUSIONS

While the semi-analytical solution procedure is computationally efficient, the fundamental physics is not solved, and as such the approach is only valid in a limited number of cases. The use of a full-thermal fluid solution procedure for the computation of the transient thermal field ensures the entire physics including the complex heat and mass transfer within advanced manufacturing processes are captured and therefore the thermal solutions these approaches generate are much more accurate and not limited to certain cases. That said the

semi-analytical solution procedure is valid in the case of EB welding where significant material is not ablated.

The utilisation of a semi-analytical solution procedure for the computation of transient thermal fields, representative of the EB welding process, coupled with a multi-phase field framework for the prediction of micro-structural evolution permits grain structure evolution near strong thermal gradients to be investigated. The effect of the thermal gradient driving force and the temperature dependent grain boundary mobility leads to the generation of columnar type grains that are oriented towards the heat source travel axis, as the thermal gradient driving force magnitude in these regions is comparable if not greater than the curvature driving force magnitude.

The effect of heat source travel speed is investigated. The higher travel speed results in a lower temperature domain on average and therefore for the same locations the boundary mobility is generally lower and the overall grain size smaller as the boundaries are not as mobile on average. The higher travel speed therefore results in a narrower heat affected zone.

ACKNOWLEDGEMENTS

The work presented in this manuscript is supported by the Engineering and Physical Sciences Research Council (EPSRC) under the "An integrated (ICME) approach to multiscale modelling of the fabrication and joining of powder processed parts" grant EP/P005284/1 and the NNUMAN programme grant in nuclear manufacturing (Grant No. EP/J021172/1).

REFERENCES

[1] XIAN-MING BAI, YONGFENG ZHANG, MICHAEL R. TONKS: *"Testing thermal gradient driving force for grain boundary migration using molecular dynamics simulations"*, Acta Materialia, pp. 95—106, 2015.

[2] ANA P FERNANDES, PRISCILA F B SOUSA, VALERIO L BORGES, GILMAR GUIMARAES: *"Use of 3D transient analytical solution based on Greens function to reduce computational time in inverse heat conduction problems"*, Applied Mathematical Modelling, pp. 4040—4049, 2010.

[3] T.F. FLINT, J.A. FRANCIS, M.C. SMITH, J. BALAKRISHNAN: *"Extension of the double-ellipsoidal heat source model to narrow-groove and keyhole weld configurations"*, Journal of Materials Processing Technology, pp. 123—135, 2017.

[4] T.F. FLINT, J.A. FRANCIS, M.C. SMITH, VASILEIOU A.N.: "*Semi-analytical solutions for the transient temperature fields induced by a moving heat source in an orthogonal domain"*, International Journal of Thermal Sciences, pp. 140—150, 2018.

[5] T.F. FLINT, C. PANWISAWAS, Y. SOVANI, M.C. SMITH, H.C. BASOALTO: *"Prediction of grain structure evolution during rapid solidification of high energy density beam induced re-melting"*, Materials & Design, pp. 200—210, 2018.

[6] THOMAS F FLINT, JOHN A FRANCIS, JOHN R YATES: *"Analytical solutions of the transient thermal field induced in finite bodies with insulating and convective boundary conditions subjected to a welding heat source"*, Conference Proceedings: SMIRT 22, San Francisco, 2013.

[7] GUNTER GOTTSTEIN, LASAR S SHVINDLERMAN: *Grain boundary migration in metals: thermodynamics, kinetics, applications*. CRC press, 2009.

[8] Y HUANG, F J HUMPHREYS: *"Measurements of grain boundary mobility during recrystallization of a single-phase aluminium alloy",* Acta Materialia, pp. 2259—2268, 1999.
[9] HYUN-KYU KIM, SEONG GYOON KIM, WEIPING DONG, INGO STEINBACH, BYEONG-JOO LEE: *"Phase-field modeling for 3D grain growth based on a grain boundary energy database"*, Modelling and Simulation in Materials Science and Engineering, pp. 34004, 2014
[10] SEONG GYOON KIM, DONG IK KIM, WON TAE KIM, YONG BUM PARK*: "Computer simulations of two-dimensional and three-dimensional ideal grain growth",* Physical Review E - Statistical, Nonlinear, and Soft Matter Physics, pp. 1—14, 2006.
[11] MATTHIAS MILITZER: *"Phase field modeling of microstructure evolution in steels",* Current Opinion in Solid State and Materials Science, pp. 106—115, 2011.
[12] CHINNAPAT PANWISAWAS, YOGESH SOVANI, RICHARD P TURNER, JEFFERY W BROOKS, HECTOR C BASOALTO, ISABELLE CHOQUET: *"Modelling of thermal fluid dynamics for fusion welding"*, Journal of Materials Processing Technology, pp. —, 2017.
[13] I STEINBACH, M APEL: *"Multi phase field model for solid state transformation with elastic strain"*, Physica D: Nonlinear Phenomena, pp. 153—160, 2006.
[14] I STEINBACH, F PEZZOLLA: *"A generalized field method for multiphase transformations using interface fields",* Physica D: Nonlinear Phenomena, pp. 385—393, 1999.
[15] B B VYNOKUR: *"Influence of alloying on the free energy of austenitic grain boundaries in steel"*, Materials Science, pp. 448—455, 1996.